

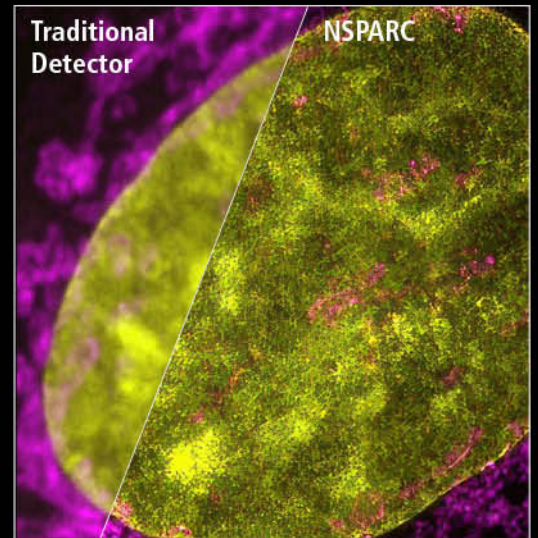


NEW

# AX / AX R with NSPARC

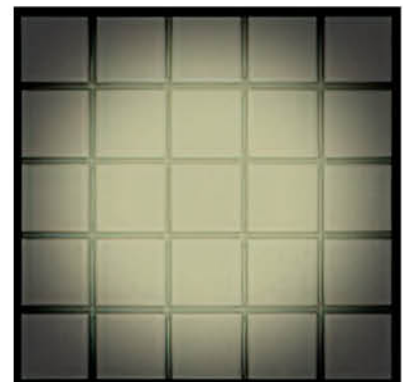
Confocal-based Super-Resolution Microscope

## Confocal Without Compromise



A New Level of Low Noise, High Sensitivity Detection

Nikon's all-new Spatial Array Confocal (NSPARC) detector for the AX/AX R confocal microscope reveals unseen details in every image, with array detection pushing the boundaries of resolution beyond the theoretical limits. NSPARC enables super-resolution via the image scanning microscopy (ISM) technique while providing a significant increase in signal-to-noise compared to traditional detectors.



Powerful Spatial Array Detector Technology

[www.microscope.healthcare.nikon.com/nsparc](http://www.microscope.healthcare.nikon.com/nsparc)

nikon-instruments-inc- nikoninstrumentsinc nikoninst nikoninstruments

Nikon Instruments Inc. • [www.microscope.healthcare.nikon.com](http://www.microscope.healthcare.nikon.com) • [nikoninstruments.us@nikon.com](mailto:nikoninstruments.us@nikon.com)

# Comparative analysis of hypoxic response of human microvascular and umbilical vein endothelial cells in 2D and 3D cell culture systems

Sandra Dienemann<sup>1</sup> | Vanessa Schmidt<sup>1</sup> | Tabea Fleischhammer<sup>1</sup> |  
Julia H. Mueller<sup>1,2</sup> | Antonina Lavrentieva<sup>1</sup> 

<sup>1</sup>Institute of Technical Chemistry, Leibniz University of Hannover, Hannover, Germany

<sup>2</sup>Department of Cardiology and Angiology, Hannover Medical School, Hannover, Germany

## Correspondence

Antonina Lavrentieva, Institute of Technical Chemistry, Leibniz University of Hannover, Hannover, Germany.

Email: [lavrentieva@iftc.uni-hannover.de](mailto:lavrentieva@iftc.uni-hannover.de)

## Funding information

This study was funded by the German Research Foundation, DFG Project 398007461 488 "Biomolecular Sensor Platform for Elucidating Hypoxic Signatures in 2D and 3D in vitro culture Systems".

## Abstract

In vitro cultivation conditions play a crucial role in cell physiology and the cellular response to external stimuli. Oxygen concentrations represent an essential microenvironmental factor influencing cell physiology and behaviour both in vivo and in vitro. Therefore, new approaches are urgently needed to monitor and control oxygen concentrations in 2D and 3D cultures, as well as cell reactions to these concentrations. In this work, we modified two types of human endothelial cells—human microvascular (huMECs) and umbilical vein endothelial cells (huVECs) with genetically encoded hypoxia biosensors and monitored cell reactions in 2D to different oxygen concentrations. Moreover, we fabricated 3D cell spheroids of different cell numbers and sizes to reveal the onset of hypoxia in huVECs and huMECs. We could demonstrate a quantitative sensor response of two cell types to reduced oxygen supply in 2D and reveal different thresholds for hypoxic response. In 3D cell spheroids we could estimate critical construct sizes for the appearance of a hypoxic core. This work for the first time directly demonstrates different hypoxic signatures for huVECs and huMECs in 2D and 3D cell culture systems.

## KEYWORDS

3D cell culture, cell spheroids, endothelial cells, huMECs, huVECs, hypoxia

## 1 | INTRODUCTION

Sufficient tissue oxygenation and nutrient supply as well as the removal of cellular decay and metabolic by-products via blood are the main functions of the circulatory system. The large vessels such as arteries, arterioles, veins and venules consist of three different layers: the *tunica intima*, *tunica media* and *tunica adventitia*. Although the exact composition differs between different types of large vessels, they all predominantly contain elastic fibres and smooth muscle cells (Tucker et al., 2022; Vajda

et al., 2021). The innermost layer of the intima is lined with endothelial cells (ECs) which form a selective barrier and are in consistent contact with blood. Small diameter vessels, also called microvasculature, lack the three-layer composition and consist only of a thin EC layer. This layer is covered by a basal lamina which has pericytes embedded (Bergers & Song, 2005). Independently of the vessel type, ECs mediate processes such as gas exchange, nutrient supply, and cellular communication between lumen and tissue to maintain tissue homeostasis (Tien, 2011; Vajda et al., 2021).

This is an open access article under the terms of the Creative Commons Attribution-NonCommercial License, which permits use, distribution and reproduction in any medium, provided the original work is properly cited and is not used for commercial purposes.

© 2023 The Authors. *Journal of Cellular Physiology* published by Wiley Periodicals LLC.

Creating a functioning vasculature in tissue engineering approaches can bridge the gap between the clinically relevant size of a potential graft and naturally occurring limitations in oxygen, nutrient supply, and waste disposal in a three-dimensional construct (Jain et al., 2005; Wang et al., 2019). The creation of a vasculature in an artificial tissue can be fabricated by both bottom-up and top-down approaches. While the bottom-up strategy describes the spontaneous self-organisation of a vascular network by ECs in a matrix, the top-down strategy uses prefabricated scaffolds seeded with ECs (Vajda et al., 2021).

Currently, human umbilical vein endothelial cells (huVECs) are the most commonly used and best characterised ECs in research due to their relatively easy isolation and the high availability of umbilical cords after childbirth. Therefore, many huVEC-based *in vitro* models for arteriosclerosis, angiogenesis, hypoxia-induced neovascularisation, and for inflammatory processes exist. Despite their widespread usage in vascularisation research, huVECs are terminally differentiated cells that exhibit their own tissue-specific phenotype and therefore do not represent a universal endothelial cell model (Jain et al., 2005; Kocherova et al., 2019; Medina-Leyte et al., 2020; Park et al., 2006). Apart from huVECs, human microvascular endothelial cells (huMECs), isolated from human foreskin, and induced pluripotent stem cell-derived endothelial cells (iPSC-ECs) are also used in vascular tissue engineering. Regardless of the originating tissue, ECs express mutual markers such as Platelet Endothelial Cell Adhesion Molecule-1 (PECAM-1 or CD31) and Von-Willebrand-Factor (vWF). Still, ECs from different origins exhibit differences in their functionality, differentiation behaviour, and cell adhesion molecules. Due to this great extent of heterogeneity, the use of tissue-specific ECs for tissue engineering seems favourable (Ades et al., 1992; Vajda et al., 2021).

Adequate oxygen supply is essential for the maintenance of cellular processes in aerobic organisms. Therefore, various physiological processes have evolved to maintain oxygen homeostasis and cope with deviating concentrations (Kietzmann et al., 2016; Majmundar et al., 2010; Michiels, 2004). Every tissue has an optimal physiological oxygen partial pressure ( $pO_2$ ) that differs throughout tissues and cell niches. The resulting  $pO_2$  is determined by the equilibrium in the oxygen supply via microvasculature and the cellular oxygen consumption. Physiological oxygen levels vary in the range between 1% and 15% oxygen. Because physiological  $pO_2$  is lower than atmospheric  $pO_2$ , it is also referred to as physiological hypoxia or physioxia. Importantly, oxygen concentrations differ not only in tissues but also in different types of vessels (e.g., veins and arteries) (Bahoun et al., 2018; Carreau et al., 2011). Traditional *in vitro* cell culture is performed under 'normoxic' conditions, which represent nearly atmospheric conditions with 95% air (containing 21% oxygen) and 5%  $CO_2$ . Considering the previously described physiological  $pO_2$ , these conditions need to be described as rather hyperoxic for most cell types (Carreau et al., 2011). Hyperoxic conditions lead to the generation of reactive oxygen species and consequently to lower metabolic activity and proliferation rates in cells (Lee & Choi, 2003). Therefore, the predictive significance with which classical 2D models

reflect physiological conditions must be questioned. Various groups have already demonstrated that huMECs show increased proliferation rates under hypoxic conditions (Decaris et al., 2009; Zhou et al., 2000). Being cells from venous skin capillaries, huMECs are physiologically exposed to oxygen tensions around 38 mmHg (5%  $pO_2$ ). In comparison, the umbilical cord vein carries less oxygenated blood with a  $pO_2$  of 20–30 mmHg (~2.6%–4%) which suggests a lower physiological oxygen concentration for the huVECs than the huMECs (Carreau et al., 2011).

In addition to the selected oxygen concentration, the cell culture geometry during cultivation has a great impact on cell behaviour. In conventional 2D cell cultivation, cells grow as an adherent monolayer with no physiologically important cell-cell or cell-ECM interactions. Providing a 3D cultivation platform, however, enables the cells to interact with each other and grow in a more *in vivo*-like microenvironment (Kapałczyńska et al., 2018; Schmitz et al., 2021). Such platforms can either be cell aggregates or a biocompatible scaffold with encapsulated cells, for example, a hydrogel. The scaffold functions as a supportive structure to imitate the natural ECM for the cells. Cell aggregates (spheroids) however, do not need an external compound since cells adhere to each other using their self-produced extracellular matrix consisting of integrins, cadherins, and glycoproteins (Schmitz et al., 2021; Weber et al., 2011). Regardless of the 3D platform, there is usually a natural oxygen and nutrient gradient toward the inner core of the construct. Oxygen is therefore, a limiting factor of the size of the 3D constructs (Däster et al., 2017; Schmitz et al., 2020). The diffusion limits for oxygen and nutrients is estimated to be at around 100–200  $\mu m$  since cells *in vivo* only survive in this range from the nearest capillary (Jain et al., 2005; Wang et al., 2019). In the absence of delivery systems, *in vitro*  $O_2$  limitations occur via low solubility at physiological temperatures and different cell densities or, in the case of aggregates, packaging density. Since every cell type reacts differently to oxygen deprivation, it is crucial to further investigate oxygen tensions that are perceived as hypoxic for this certain cell type in 2D and 3D (Schmitz et al., 2021).

The usage of genetically encoded fluorescence biosensors provides direct information about the cells' reaction to specific conditions or treatments. In this study, a hypoxia sensor, first reported by Erapanedi et al. (Erapanedi et al., 2016), was used to visualise the physiological cell response to hypoxia caused by either oxygen displacement in the incubator in 2D cell cultures or by natural oxygen gradients in 3D spheroids. Due to the oxygen independent maturation of the reporter protein UnaG, its usage as a hypoxia sensor is advantageous to classic fluorescence reporters such as the green fluorescence protein (GFP) (Erapanedi et al., 2016; Kumagai et al., 2013). The reporter construct encodes the UnaG fluorescence protein that is under the same transcriptional control as the hypoxia response elements (HREs). The stabilisation of Hypoxia-inducible factor 1 $\alpha$  (HIF-1 $\alpha$ ) during hypoxia enables the transcriptional activation of HRE and therefore a HIF-1 $\alpha$  dependent expression of the UnaG fluorescence protein. Earlier we could demonstrate that Mesenchymal Stem/Stromal Cells (MSCs) modified with these

sensors provide quantitative fluorescence signal depending on O<sub>2</sub> concentrations (Schmitz et al., 2020).

In this study we used huVECs and huMECs, modified with a genetically encoded hypoxia sensor system to study differences in their response to hypoxia. We performed a comparative study of the hypoxia onset of both cell types in 2D cell culture under the influence of different oxygen levels. Furthermore, we investigated the formation of a hypoxic core in 3D spheroid cell aggregates depending on different cell-seeding densities.

## 2 | MATERIALS AND METHODS

### 2.1 | Hypoxia reporter huVECs and huMECs

The via CI-SCREEN technology immortalised huVEC and huMEC cell lines were obtained from InSCREENeX GmbH and lentivirally transduced with hypoxia biosensors as described by Schmitz et al. (Schmitz et al., 2020). Lateral flow tests Lenti-X<sup>TM</sup> GoStix<sup>TM</sup> Plus (TaKaRa Bio Inc) were used to ensure that the same amount of virus was used for both cell types. Cells were cultivated in gelatine-coated (0.5% gelatine) cell culture T-flasks with either huVEC or huMEC medium (InSCREENeX GmbH) supplemented with 6% supplements (InSCREENeX GmbH) and 50 µg/mL gentamicin (Merck KGaA). Cells were subcultivated one to two times a week when reaching a confluency of 90%. For passaging the cells, the medium was removed and the cells were washed with phosphate-buffered saline (PBS) and detached by accutase (Merck KGaA) treatment. Reseeding density was  $1 \times 10^4$  cells per cm<sup>2</sup>. For all experiments passages 17 to 29 of both cell types were used. Furthermore, both cell types were tested for specific cell markers CD31, CD34, CD45 in passage 27. The cells were cultivated in 2D and harvested by accutase treatment. For each marker  $10 \times 10^4$  cells were placed in a reaction tube, pelleted and resuspended in 100 µL cold blocking buffer (PBS supplemented with 2% human serum [CC-pro]). In total 2 µL of the respective antibody BD Pharmingen<sup>TM</sup> conjugated with either FITC or PE-CF594 (Becton Dickinson) was added to the reaction tubes and the cell suspensions were incubated at room temperature for 20 min in the dark. Afterwards, another 400 µL of blocking buffer and 1 µL propidium iodide (50 µg/mL) were added and again incubated at room temperature for 5 min. Cells were filtrated through a 70 µm cell strainer (VWR International GmbH) and measured in the BD Accuri<sup>TM</sup> C6 (Becton Dickinson). For FITC and UnaG detection the FL1 (533/30 nm), for PE-CF594 the FL3 (>670 nm) and for propidium iodide the FL2 (585/40 nm) filters of the Solid State Blue Laser were used.

### 2.2 | Cultivation under reduced oxygen tensions

To investigate the cell response to low oxygen concentrations ranging from 1% to 5%, the cells were harvested by accutase treatment and seeded in triplicates in gelatine-coated six-well-plates (Sarstedt) at a density of  $5 \times 10^4$  cells per well in 2 mL medium

containing 10% human serum (CC-pro). Afterwards, the cells were incubated for 24 h at 21% O<sub>2</sub> to adhere and then the well plates were transferred into the oxygen control incubator C16 (Labotect Labor-Technik-Göttingen GmbH) that displaces oxygen with N<sub>2</sub>. The CO<sub>2</sub> level was kept at 5% and temperature at 37°C. After 24 h and 48 h under reduced oxygen tensions, cells were detached and the fluorescence signal was quantified by flow cytometry. The remaining cells were returned to 21% O<sub>2</sub> and measurements were carried out directly after exposing the cells to 24 h or 48 h of reduced oxygen tensions as well as 24 h or 48 h after reoxygenation at 21% O<sub>2</sub>.

### 2.3 | 3D spheroid formation

To fabricate spheroids of different cell numbers, cells were expanded in 2D as described above, harvested, and counted in a Neubauer haemocytometer. The required cell numbers were pelleted and resuspended in the respective basal medium supplemented with 10% human serum, 6% supplements and 50 µg/mL gentamicin. Cells were then seeded in a total volume of 150 µL per well in 96-well Sarstedt Biofloat<sup>TM</sup> ultra-low attachment plates (Sarstedt) resulting in cell numbers ranging from 0.5 to  $30 \times 10^4$  cells per well. Spheroids were cultivated up to 48 h at 21% O<sub>2</sub>, 5% CO<sub>2</sub> and 37°C. After 24 h as well as after 48 h, three spheroids of each cell number were transferred to lumox<sup>®</sup> multiwell plates and the fluorescence signal was documented using the Cytation<sup>®</sup>5 Cell imaging multimode reader (Agilent Technologies). The diameter of the spheroids and their hypoxic cores were measured in both x- and y-axis using the Gen5 3.10 software (Agilent Technologies).

### 2.4 | Flow cytometry and microscopy

For flow cytometric analysis, the BD Accuri<sup>TM</sup> C6 was used. The adherent cells were harvested using accutase treatment, pelleted and resuspended in PBS for measurement. Spheroids were washed with PBS and transferred to 2 mL reaction tubes for dissociation via TrypLE<sup>TM</sup> Select Solution 10x (Thermo Fisher) treatment at 37°C. TrypLE<sup>TM</sup> was diluted 1:2 in PBS and 200 µL were added to each spheroid sample. Every 2 min, the spheroids were mechanically disrupted by pipetting using low retention filter tips. After full digestion of the spheroid (5–10 min), the cells were pelleted and resuspended in PBS for the flow cytometric measurements. The cell suspension was filtrated through a 70 µm cell strainer to separate single cells for measurement. The gated population was excited by a Solid State Blue Laser at 488 nm and the resulting green fluorescence was detected with the FL1 (533/30 nm) detector.

Fluorescence microscopy was carried out using the BioTek Cytation<sup>®</sup>5 Cell imaging multimode reader. For UnaG fluorescence detection, the GFP filter cube (469/525 nm) was used. Multiple images of the 3D constructs such as the spheroids and hydrogel discs were taken along the entire x-, y- and z-axis and stitched together using the montage as well as z-stacking function in the Gen5 3.10 software.

For time lapse videos the Incucyte<sup>®</sup> S3 Live-Cell Imaging System (Sartorius) was used. Pictures of the spheroids were taken every 10 min in the Brightfield and Green channel and exported as videos with 15 fps. The dynamics of the hypoxic core formation was analysed via 'Largest Brightfield Object Green Integrated Intensity' in the Incucyte<sup>®</sup> software.

## 2.5 | Statistical analysis

For graphical representation of the data and statistical analysis OriginPro<sup>®</sup> 2021 (OriginLab) was used. Various plots represent the mean  $\pm$  SD ( $n = 3$ ). The data was tested via Shapiro-Wilk test for normal distribution. For normal distributed data a one-way analysis of variance (ANOVA) with a post hoc Bonferroni correction was used. For non-normally distributed a Mann-Whitney-test was performed. A  $p < 0.05$  was considered as statistically significant.

## 3 | RESULTS

### 3.1 | Creation and characterisation of hypoxia sensor-modified huVECs and huMECs

The HRE-dUnaG hypoxia sensor construct was integrated into the genome of both huVEC and huMEC via lentiviral transduction. Afterwards, the modified cells were quarantined for 2 weeks until no virus particles were detectable. To determine the efficiency of transduction, the cells were incubated in both normoxia (21% O<sub>2</sub>) and hypoxia (1% O<sub>2</sub>) for 24 h and the fluorescence was quantified by flow cytometry. For huVECs, a 26-fold increase in fluorescence for

97.47% of the cells due to activation of the hypoxia sensor was detected. huMECs showed fluorescence in 96.1% of the cells with an increase by 35-fold (Supporting Information: S1). For both cell types, fluorescence was also verified microscopically (Figure 1). To ensure the identity of modified huVECs and huMECs, cells were tested for various surface antigens. Table 1 represents the result of analysis and corresponding flow cytometric profiles shown in the Supporting Information: S2.

### 3.2 | Hypoxic response in 2D

The reporter cells were cultivated in six different oxygen concentrations (1%, 1.5%, 2%, 2.5%, 5% and 21% O<sub>2</sub>) for either 24 h or 48 h to determine a threshold for both cell types at which HIF-1 $\alpha$  is stabilised as a cellular response to oxygen deprivation and to quantify the hypoxic response. The fluorescence was analysed by microscopy and quantified by flow cytometry (Figure 2). For both huVECs and huMECs, the measured hypoxic reporter response was in direct correlation with the O<sub>2</sub> concentration set in the incubator.

**TABLE 1** Summarised surface antigen expression profile of modified huMECs and huVECs.

Marker	Expression in huVECs [%]	Expression in huMECs [%]
CD31	92.3	88.6
CD45	0.6	0.3
CD34	0.7	0.3

Abbreviations: huMECs; human microvascular endothelial cells; huVECs, human umbilical vein endothelial cells.

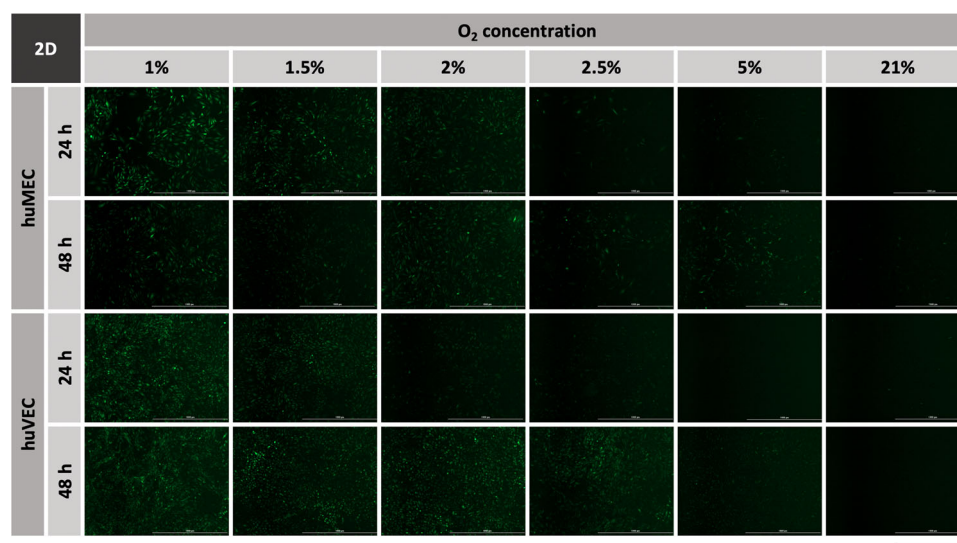


**FIGURE 1** Comparison of hypoxia-reporter huMECs and huVECs in 2D cell culture in different oxygen concentrations (1%, 1.5%, 2%, 2.5%, 5%, 21%). Fluorescence microscopic analysis of UnaG expression using Cytation<sup>®</sup>5 after 24 h and 48 h cultivation at designated oxygen concentrations. Seeding density  $5 \times 10^4$  cells/cm<sup>2</sup>. Scale bar 1000  $\mu$ m. huMECs; human microvascular endothelial cells; huVECs, Human umbilical vein endothelial cells.

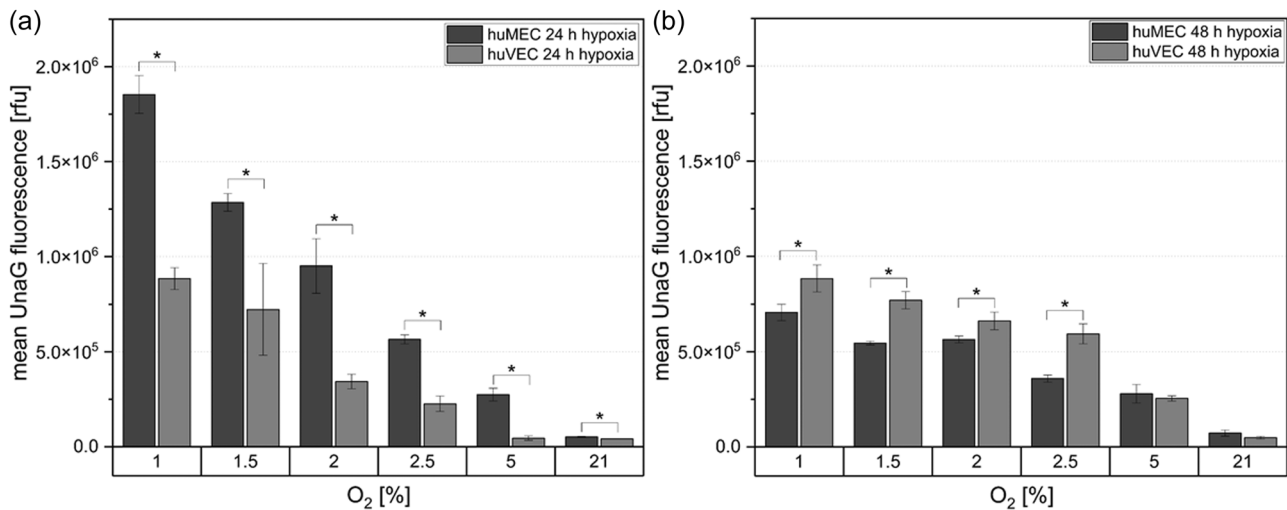


**FIGURE 2** Comparison of hypoxia-reporter huMECs and huVECs in 2D cell culture in different oxygen concentrations (1%, 1.5%, 2%, 2.5%, 5%, 21%). (a) mean single cell fluorescence of huMEC and huVEC hypoxia-reporter cells determined by flow cytometry after 24 h hypoxia with X% O<sub>2</sub>. (b) mean single cell fluorescence of huMEC and huVEC hypoxia-reporter cells determined by flow cytometry after 48 h hypoxia with X% O<sub>2</sub>. Data show mean ± SD of a 3-fold determination, \**p* < 0.05. huMECs; human microvascular endothelial cells; huVECs, Human umbilical vein endothelial cells.

After 24 h of hypoxia, the hypoxic response of the huMECs was twice as high as the response of the huVECs (Figure 2a). Since no elevated fluorescent UnaG reporter signal could be detected for the huVECs after 24 h with 5% O<sub>2</sub>, the threshold for the hypoxic response of this cell type is in the range between 2.5% and 5% O<sub>2</sub>. For huMECs, the threshold has to be above 5% O<sub>2</sub> due to the clear fluorescence signal at 5%. The same experiment was conducted for a prolonged period of 48 h hypoxia to study the dynamics of the sensor fluorescence. The data (Figure 2b) show, similar to 24 h of hypoxia, a reduction in the reporter signal intensity with increasing oxygen; however, while huVECs maintain or even increase reporter fluorescence intensity, the signal of the huMECs falls to lower values than for the huVECs. After hypoxia the cells were further cultivated for 48 h in 21% O<sub>2</sub> to monitor the reduction of the fluorescence signal during reoxygenation. The lower the previous oxygen concentration, the faster the reduction of the fluorescence signal during reoxygenation (Supporting Information: S3). For both cell types and all O<sub>2</sub> concentrations there was no reporter UnaG signal detectable after 48 h at 21% O<sub>2</sub>.

### 3.3 | Hypoxic response in 3D spheroids

To investigate the hypoxic response of huVECs and huMECs in 3D in a more in vivo-like microenvironment, spheroids of various cell numbers (0.5, 1, 3, 7.5, 15, 30 × 10<sup>4</sup> cells/spheroid) were fabricated using ultra low attachment plates. The influence of the cell number on the spheroid size as well as its hypoxic core due to reduced oxygen diffusion inside the construct were investigated over a period of 48 h. The measurement of spheroid diameters showed an increase

in size in correlation to the cell number. After 24 h of cultivation, huVEC cell spheroids were slightly smaller in size than huMEC spheroids of the same cell numbers. After 48 h of cultivation, spheroid diameters of both cell types decreased, indicating denser packaging (Figure 3). For both cell types, no fluorescence of the UnaG hypoxia sensor could be detected in the smallest spheroids (0.5 × 10<sup>4</sup> cells). However, starting from 1 × 10<sup>4</sup> cells, huVEC spheroids showed a fluorescent hypoxic core surrounded by a layer of nonhypoxic cells. Fluorescence microscopy demonstrated higher reporter signal intensity in huVEC spheroids when compared to huMEC spheroids of similar cell numbers.

The hypoxic fraction of the total diameter increased with increasing spheroid size and was consistently larger in huMECs than in huVECs. Spheroids of both cell types, however, developed a nonhypoxic core indicating dead cells for the larger investigated spheroid sizes starting from 7.5 × 10<sup>4</sup> cells for huVECs and 15 × 10<sup>4</sup> for huMECs (Figure 4).

To quantify and compare hypoxic response of huVECs and huMECs in 3D, spheroids were additionally dissociated and cell fluorescence was measured by flow cytometry (Figure 5). Quantification of the fluorescent signal supported the results observed by microscopy, but also revealed that for the same spheroid sizes huVECs in 3D demonstrate a stronger hypoxic response than huMECs.

Time lapse analysis of the fluorescence onset in the spheroids of both cell types also revealed higher fluorescence in huVEC spheroids (Figure 6 and time lapse videos in Supporting Information: S4) than in huMECs. huVEC spheroids of the same cell numbers had a faster increase and higher integrated fluorescence intensity in comparison to huMECs.

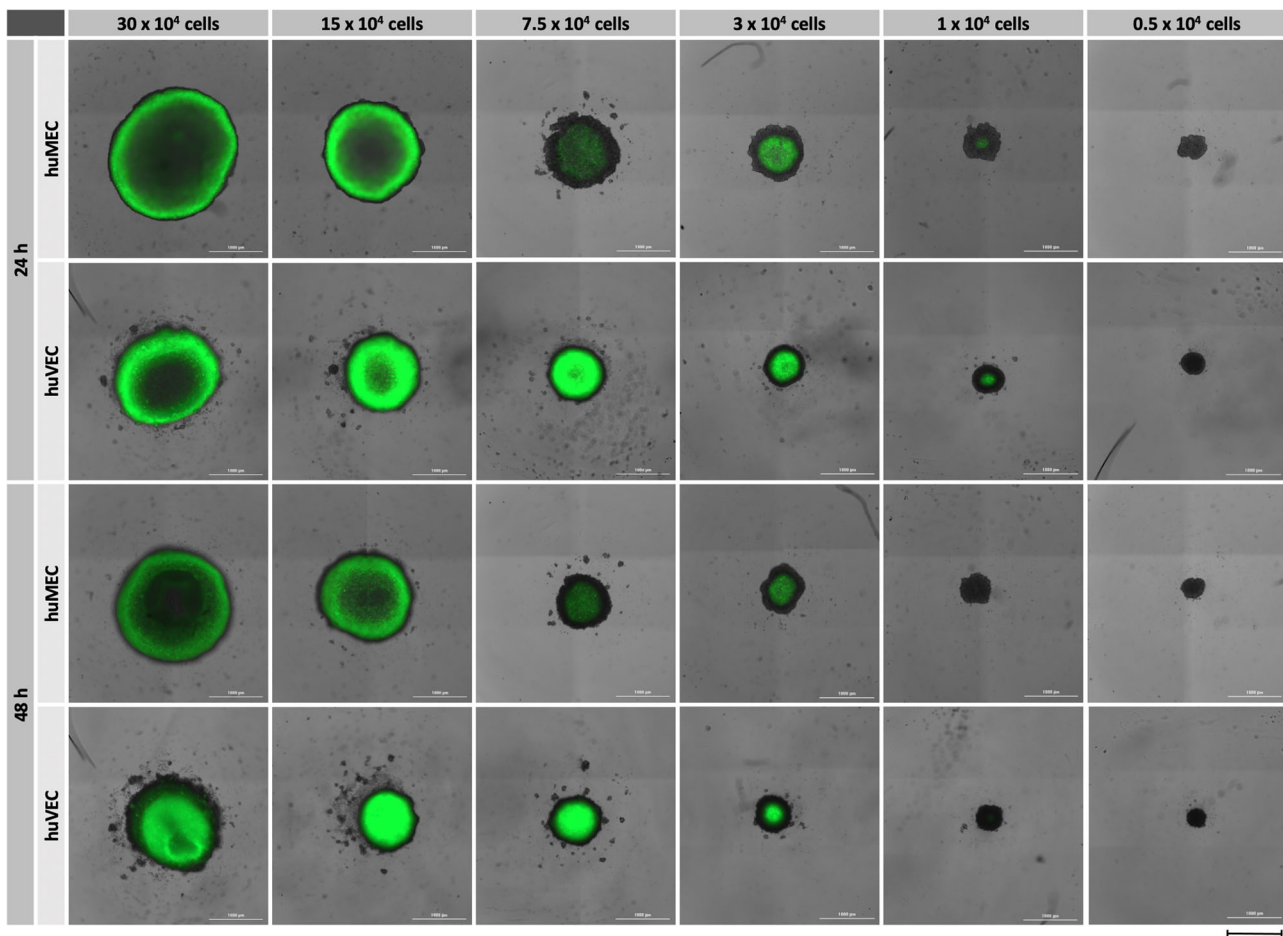


**FIGURE 3** Comparison of the hypoxic response of huMEC and huVEC spheroids with different cell numbers after 24 h and 48 h incubation at 37°C and 21% O<sub>2</sub>. Overlay of fluorescence and Brightfield microscopy. Scale bar 1000 μm. huMEC; human microvascular endothelial cell; huVEC, Human umbilical vein endothelial cell.

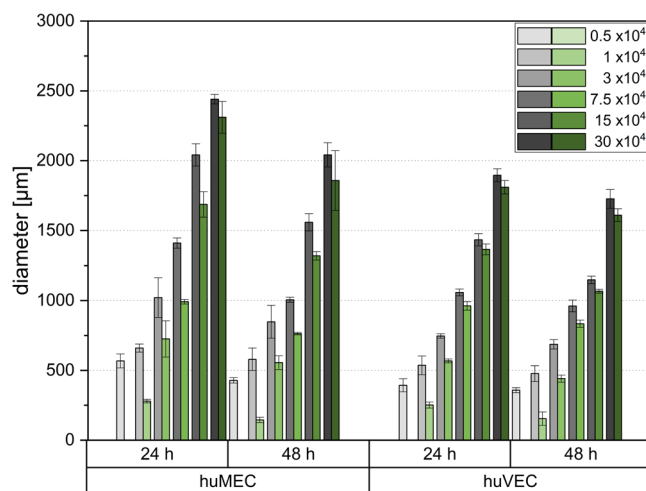


**FIGURE 4** Mean diameter of the spheroids (grey) and their fluorescent hypoxic core (green) for all tested cell numbers after 24 h and 48 h of incubation. Data show mean ± SD of a 3-fold determination, measured in Gen5 3.10 software.

## 4 | DISCUSSION AND CONCLUSIONS

Endothelial cells isolated from various sources are widely used in basic research and regenerative medicine. On the one hand, they can be used to better understand molecular mechanisms involved in physiological processes of angiogenesis, as well as for the screening of antiangiogenic compounds (Arnaoutova & Kleinman, 2010). On the other hand, they are considered promising candidates for the prevascularisation of tissue engineering constructs (Laschke & Menger, 2016). In fact, several potential approaches have been reported in which prevascularised constructs were able to improve cell survival after implantation (Gholobova et al., 2020; Laschke & Menger, 2016). Another rapidly growing area of research in recent years is 3D cell culture, which provides a physiologically relevant cell environment and, as a result, in vivo-like cell behaviour. Here, the advantages of 3D cell culture systems can be used for the development of relevant in vitro models for research and drug screening (Langhans, 2018; Sambale et al., 2015). As the simplest and most cost-effective technique, scaffold-free cell aggregates are becoming one of the most popular 3D platforms (Sambale et al., 2015). Numerous in

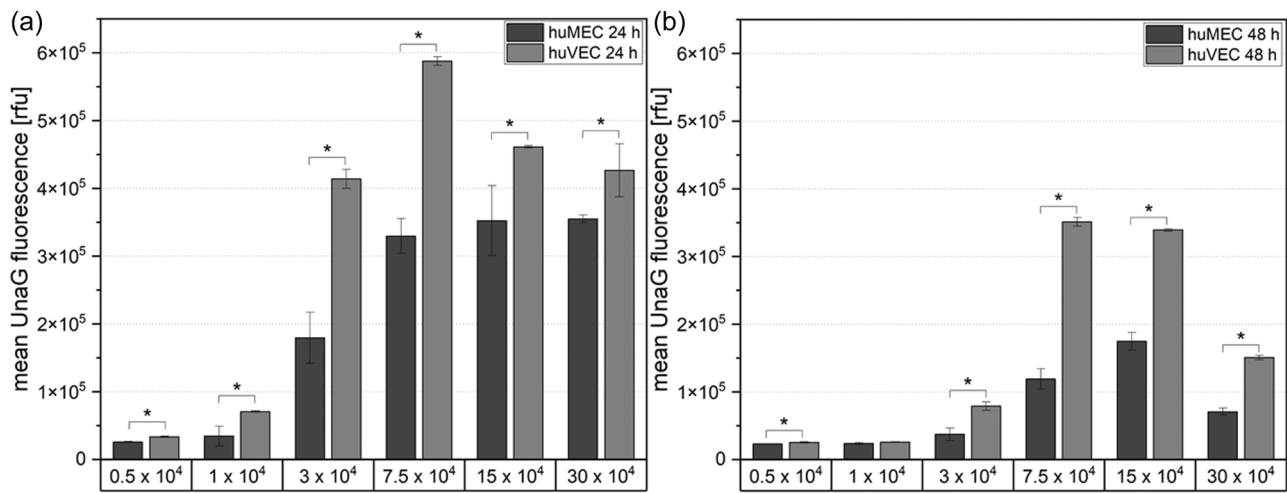


**FIGURE 5** Hypoxic response of huMECs and huVECs in 3D spheroids. Flow cytometric analysis of the hypoxic response of huMEC and huVEC 3D spheroids with different cell numbers after (a) 24 h and (b) 48 h incubation at 37°C and 21% O<sub>2</sub>. Data show mean ± SD of a 3-fold determination, \**p* < 0.05. huMECs; human microvascular endothelial cells; huVECs, Human umbilical vein endothelial cells.

vitro models and assays using 3D spheroids composed of endothelial cells have been reported, demonstrating the broad applicability of this system (Laschke & Menger, 2017). Another important parameter of in vitro cell cultivation is the level of dissolved oxygen (Bahsoun et al., 2018). Local oxygen concentrations represent the balance between supply and consumption and most tissues have naturally lower oxygen tensions than the 21% O<sub>2</sub> which is typically used for cell cultures in vitro (Ivanovic, 2009). In addition, under pathological conditions (e.g., infections or wounds), the oxygen content in tissues decreases even further (Luo et al., 2022). All of the above shows the importance of precise knowledge and control of the cultivation conditions for medically relevant cell systems.

The aim of the present study was to better understand hypoxic reactions of endothelial cells derived from umbilical vein (huVECs) and from dermal capillaries (huMECs) in 2D and 3D cultivation systems. HuVECs are the most popular endothelial cells, since they can be easily obtained from umbilical cords after delivery. Moreover, they demonstrate high proliferation capacities and the ability to form capillary networks under controlled conditions (Vajda et al., 2021). HuMECs are more difficult to isolate, but also used to study angiogenesis in norm and disease (Ades et al., 1992). Although both cell types demonstrate the same characteristics in terms of specific marker expression for example, the origin of these cells and consequently native physiological milieus are completely different (Vajda et al., 2021). While huMECs are normally exposed to oxygen concentrations of 38 mmHg (5% O<sub>2</sub>), huVECs function and grow at lower oxygen tensions (20–30 mmHg, or 2.6%–4% O<sub>2</sub>) as they serve as the lining of umbilical veins that carry deoxygenated blood from the foetus to the placenta (Carreau et al., 2011).

The implementation of genetically encoded hypoxia biosensors to directly monitor cellular hypoxia response has proven to be a reliable tool for 2D and 3D cell cultures (Schmitz et al. 2020, 2021). Moreover, the response of the fluorescence sensor was directly

related to oxygen concentrations—the lower the oxygen tension, the higher the reporter fluorescence (Schmitz et al., 2020). Thus, with the help of this biosensor, a quantitative cellular reaction to hypoxia could be detected. After integration of the hypoxia biosensor, both cell types were characterised with the help of flow cytometric analysis for the specific endothelial marker expression. Modified cells modified with the hypoxia sensor retained a specific marker expression profile, being positive for endothelial marker (CD31) and negative for hematopoietic markers (CD34, CD45).

After characterisation, huVECs and huMECs were exposed to various oxygen concentrations (1%, 1.5%, 2%, 2.5% and 5% O<sub>2</sub>) for 24 h and 48 h in 2D cell cultures. Similar to the results obtained earlier with mesenchymal stem cells, the hypoxic response increased with decreased oxygen concentration (Schmitz et al., 2020). HuVECs, however, demonstrated a lower fluorescent signal over all tested hypoxic conditions and lower hypoxic sensor onset threshold (2.5% O<sub>2</sub>) if compared to huMECs (5% O<sub>2</sub>). Hypoxic response in huVECs and the threshold of HIF-1α stabilisation observed in this study was similar to the results of Keeley et al. who performed Western Blot analysis for the detection of HIF-1α stabilisation and identified its stabilisation at 3% O<sub>2</sub> (Keeley et al., 2017). Lower in vivo oxygen tension measured in umbilical cord vein indicates that the normal physiological O<sub>2</sub> range for these cells is lower than the one for huMECs. That means that huVECs and huMECs have different thresholds for HIF-1α stabilisation and thus, different cellular reactions in vivo and in vitro at low oxygen concentrations. Being the widespread model for vascularisation, huVECs, however, seem not to be a perfect cellular candidate to study vascularisation in tissues where higher oxygen levels are observed. On the other hand, these cells can survive better after implantation alone or as a part of the tissue engineered construct, since huVECs are less sensitive to oxygen deprivation. Nevertheless, this study for the first time directly demonstrates that endothelial cells derived from different vessels have unequal reaction on lower oxygen levels.



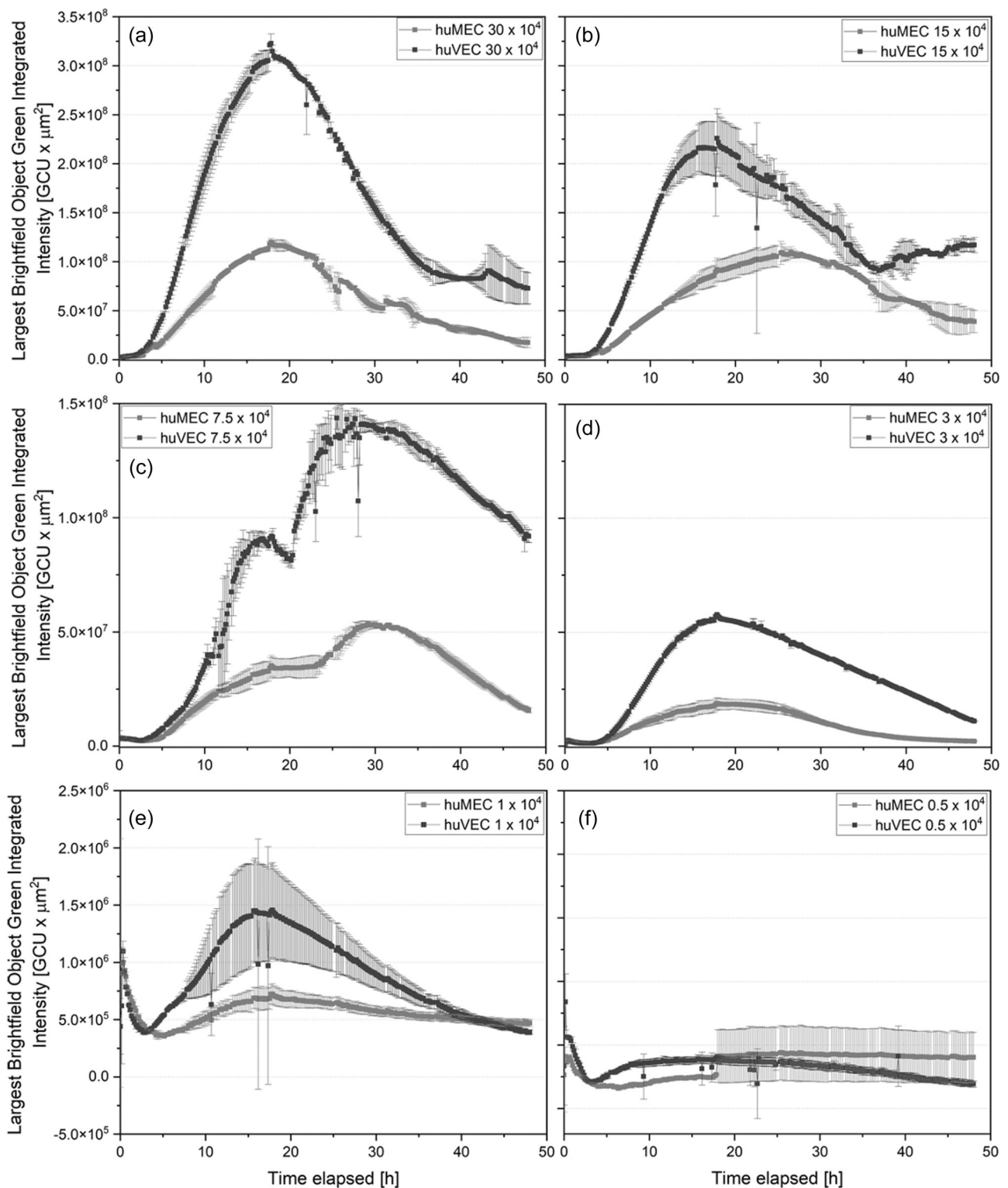


**FIGURE 6** Hypoxic sensor response dynamics analysed by the Incucyte<sup>®</sup> S3 Live-Cell Imaging System and Software (Sartorius). (a)  $30 \times 10^4$  cells/spheroid (b)  $15 \times 10^4$  cells/spheroid (c)  $7.5 \times 10^4$  cells/spheroid (d)  $3 \times 10^4$  cells/spheroid (e)  $1 \times 10^4$  cells/spheroid (f)  $0.5 \times 10^4$  cells/spheroid. Data show mean  $\pm$  SD of a 2-fold determination.

In the second part of the study, we evaluated the hypoxic response of both cell types in 3D cell spheroids. Spheroids of different cell numbers were fabricated ( $0.5$ ,  $1$ ,  $3$ ,  $7.5$ ,  $15$  and  $30 \times 10^4$  cells per spheroid) and the onset of hypoxic responses was detected by fluorescent microscopy, time

lapse microscopy and flow cytometry of dissociated spheroids. As it can be seen from microscopy analysis and corresponding time lapse videos, first HIF-1 $\alpha$  stabilisation with corresponding detected fluorescent reporter signal was observed in spheroids with  $1 \times 10^4$  cells and a

diameter of 550  $\mu\text{m}$ . This spheroid size and cell numbers are bigger than earlier believed 300  $\mu\text{m}$  (Hirschhaeuser et al., 2010; Land & Rae, 2005). This can be explained by the fact that most of the studies on the hypoxic core in spheroid cultures were initially performed on cancer cell lines, which have altered cellular metabolism. Interestingly, a clear hypoxic core surrounded by non-hypoxic cells was detected in each spheroid in both studied cell types. The size of the hypoxic core increased with spheroid size. Compared to previously studied MSCs spheroids, huVEC and huMEC spheroids demonstrate a clear boundary between the hypoxic core and non-hypoxic shell (Schmitz et al., 2021). Fluorescence intensity, however, seemed to be higher in huVEC aggregates of the same size when compared to huMECs. Following spheroid dissociation and flow cytometric measurements supported the results of microscopy, demonstrating increasing reporter fluorescence with growing spheroid sizes. Surprisingly, hypoxic response of huVECs in 3D spheroids was stronger than the one for the huMEC spheroids, while in 2D cell cultures huVECs reacted at the same low oxygen concentrations with weaker response. One explanation here could be the packaging density of huVEC spheroids, which were smaller in diameter than huMEC spheroids of the same cell numbers (Figure 4). We can also speculate that culturing huVECs and huMECs in a 3D environment shows a different cellular response compared to nonphysiological 2D cell cultures. Indeed, different cellular responses to hypoxia have already been found in 3D culture systems compared to hypoxic 2D cultures (DeiNero et al., 2015).

For both studied cell types, sensor fluorescence decreased after 48 h both in 2D and 3D cultures. Decrease of fluorescence can be a consequence of cellular adaptation to hypoxia. Indeed, HIF-1 $\alpha$  stabilisation (which is detected by this type of sensor) is the result of cellular response to acute hypoxia, followed by increased involvement of HIF-2 $\alpha$ , which is responsible for the cells reaction to prolonged hypoxia (Bahsoun et al., 2018; Bartoszewski et al., 2019). Bartoszewski et al. studied the switch of HIF-1 $\alpha$  to HIF-2 $\alpha$  in endothelial cells of different origins, cultivated in 2D under 0.9% O<sub>2</sub>. They revealed a decrease up to full disappearance of HIF-1 $\alpha$  and an increase of HIF-2 $\alpha$  accumulation over 48 h in huVECs. For dermal huMECs, an even faster switch from HIF-1 $\alpha$  to HIF-2 $\alpha$  was detected (Bartoszewski et al., 2019). Furthermore, it was demonstrated that in comparison to other cell types, in ECs, HIF-2 $\alpha$  transcriptionally regulates a larger set of target genes compared with those of HIF-1 $\alpha$  (Downes et al., 2018). Future development and application of genetically encoded HIF-2 $\alpha$  biosensors will help to monitor and understand better the HIF-1 $\alpha$  to HIF-2 $\alpha$  switch in 2D and 3D cell cultures.

Taken together, our data indicate that endothelial cell origin may play an important role in cellular responses to hypoxia. The next crucial parameter affecting cell responses is the cultivation platform—here we have shown that the hypoxic response can be different for 2D and 3D cell cultures. We demonstrated that different cultivation conditions result in different hypoxic responses and, consequently, alternated cell states and reactions. For the first time, the hypoxic response of huVECs and huMECs was monitored directly in 2D and 3D cultivation systems. Moreover, the reporter cells created in this work can be used as a reliable transferable toolkit for further studies,

for example, in bioprinting, characterisation of novel biomaterials or disease modelling. Using these reporter cells, critical sizes for in vitro constructs can be identified, in the case of intended hypoxic 3D in vitro models, the presence of a hypoxic cell state can be documented and the efficacy of vascularisation or other oxygen delivery strategies in tissue engineered constructs can be directly assessed.

## AUTHOR CONTRIBUTIONS

**Antonina Lavrentieva:** Conceptualisation; writing—review and editing; supervision; funding acquisition. **Sandra Dienemann:** Conceptualisation; development of methodology, experiment performance and data analysis; writing—original draft preparation; writing—review and editing. **Julia H. Mueller:** Development of methodology, experiment performance and data analysis. **Vanessa Schmidt:** Development of methodology, experiment performance and data analysis. **Tabea Fleischhammer:** Writing—review and editing. All authors have read and agreed to the published version of the manuscript.

## ACKNOWLEDGEMENTS

We would like to thank Vsevolod V. Belousov and Ekaterina Potekhina for providing sensor plasmids. We also thank Christopher Bartram, Marline Kirsch and Guillem Vernet Armengol for their help with data analysis. Open Access funding enabled and organized by Projekt DEAL. This study was funded by the German Research Foundation, DFG Project 398007461 488 'Biomolecular Sensor Platform for Elucidating Hypoxic Signatures in 2D and 3D in vitro culture Systems'.

## CONFLICT OF INTEREST STATEMENT

The authors declare no conflict of interest.

## ORCID

Antonina Lavrentieva  <http://orcid.org/0000-0003-0003-5572>

## REFERENCES

- Ades, E. W., Candal, F. J., Swerlick, R. A., George, V. G., Summers, S., Bosse, D. C., & Lawley, T. J. (1992). HMEC-1: Establishment of an immortalized human microvascular endothelial cell line. *Journal of Investigative Dermatology*, 99(6), 683–690.
- Arnautova, I., & Kleinman, H. K. (2010). In vitro angiogenesis: Endothelial cell tube formation on gelled basement membrane extract. *Nature Protocols*, 5(4), 628–635.
- Bahsoun, S., Coopman, K., Forsyth, N. R., & Akam, E. C. (2018). The role of dissolved oxygen levels on human mesenchymal stem cell culture success, regulatory compliance, and therapeutic potential. *Stem Cells and Development*, 27(19), 1303–1321.
- Bartoszewski, R., Moszyńska, A., Serocki, M., Cabaj, A., Polten, A., Ochocka, R., Dell'Italia, L., Bartoszewski, S., Króliczewski, J., Dąbrowski, M., & Collawn, J. F. (2019). Primary endothelial cell-specific regulation of hypoxia-inducible factor (HIF)-1 and HIF-2 and their target gene expression profiles during hypoxia. *The FASEB Journal*, 33(7), 7929–7941.
- Bergers, G., & Song, S. (2005). The role of pericytes in blood-vessel formation and maintenance. *Neuro-Oncology*, 7(4), 452–464.
- Carreau, A., Hafny-Rahbi, B. E., Matejuk, A., Grillon, C., & Kieda, C. (2011). Why is the partial oxygen pressure of human tissues a crucial parameter? Small molecules and hypoxia. *Journal of Cellular and Molecular Medicine*, 15(6), 1239–1253.

- Däster, S., Amatruda, N., Calabrese, D., Ivanek, R., Turrini, E., Droeser, R. A., Zajac, P., Fimognari, C., Spagnoli, G. C., Iezzi, G., Mele, V., & Muraro, M. G. (2017). Induction of hypoxia and necrosis in multicellular tumor spheroids is associated with resistance to chemotherapy treatment. *Oncotarget*, *8*(1), 1725–1736.
- Decaris, M. L., Lee, C. I., Yoder, M. C., Tarantal, A. F., & Leach, J. K. (2009). Influence of the oxygen microenvironment on the proangiogenic potential of human endothelial colony forming cells. *Angiogenesis*, *12*(4), 303–311.
- DelNero, P., Lane, M., Verbridge, S. S., Kwee, B., Kermani, P., Hempstead, B., Stroock, A., & Fischbach, C. (2015). 3D culture broadly regulates tumor cell hypoxia response and angiogenesis via pro-inflammatory pathways. *Biomaterials*, *55*, 110–118.
- Downes, N. L., Laham-Karam, N., Kaikkonen, M. U., & Ylä-Herttua, S. (2018). Differential but complementary HIF1 $\alpha$  and HIF2 $\alpha$  transcriptional regulation. *Molecular Therapy*, *26*(7), 1735–1745.
- Erapaneedi, R., Belousov, V. V., Schäfers, M., & Kiefer, F. (2016). A novel family of fluorescent hypoxia sensors reveal strong heterogeneity in tumor hypoxia at the cellular level. *The EMBO Journal*, *35*(1), 102–113.
- Gholobova, D., Terrie, L., Mackova, K., Desender, L., Carpentier, G., Gerard, M., Hympanova, L., Deprest, J., & Thorrez, L. (2020). Functional evaluation of prevascularization in one-stage versus two-stage tissue engineering approach of human bio-artificial muscle. *Biofabrication*, *12*(3), 035021.
- Hirschhaeuser, F., Menne, H., Dittfeld, C., West, J., Mueller-Klieser, W., & Kunz-Schughart, L. A. (2010). Multicellular tumor spheroids: An underestimated tool is catching up again. *Journal of Biotechnology*, *148*(1), 3–15.
- Ivanovic, Z. (2009). Hypoxia or in situ normoxia: The stem cell paradigm. *Journal of Cellular Physiology*, *219*(2), 271–275.
- Jain, R. K., Au, P., Tam, J., Duda, D. G., & Fukumura, D. (2005). Engineering vascularized tissue. *Nature Biotechnology*, *23*(7), 821–823.
- Kapałczyńska, M., Kolenda, T., Przybyła, W., Zajączkowska, M., Teresiak, A., Filas, V., Ibbs, M., Bliźniak, R., Łuczewski, Ł., & Lamperska, K. (2018). 2D and 3D cell cultures—A comparison of different types of cancer cell cultures. *Archives of Medical Science: AMS*, *14*(4), 910–919.
- Keeley, T. P., Siow, R. C. M., Jacob, R., & Mann, G. E. (2017). A PP2A-mediated feedback mechanism controls Ca<sup>2+</sup>-dependent NO synthesis under physiological oxygen. *The FASEB Journal*, *31*(12), 5172–5183.
- Kietzmann, T., Mennerich, D., & Dimova, E. Y. (2016). Hypoxia-inducible factors (HIFs) and phosphorylation: Impact on stability, localization, and transactivity. *Frontiers in Cell and Developmental Biology*, *4*, 11.
- Kocherova, I., Bryja, A., Mozdziaż, P., Angelova Volponi, A., Dyszkiewicz-Konwińska, M., Piotrowska-Kempisty, H., Antosik, P., Bukowska, D., Bruska, M., Iżycki, D., Zabel, M., Nowicki, M., & Kempisty, B. (2019). Human umbilical vein endothelial cells (HUVECs) co-culture with osteogenic cells: From molecular communication to engineering prevascularised bone grafts. *Journal of Clinical Medicine*, *8*(10), 1602.
- Kumagai, A., Ando, R., Miyatake, H., Greimel, P., Kobayashi, T., Hirabayashi, Y., Shimogori, T., & Miyawaki, A. (2013). A bilirubin-inducible fluorescent protein from eel muscle. *Cell*, *153*(7), 1602–1611.
- Land, S. C., & Rae, C. (2005). iNOS initiates and sustains metabolic arrest in hypoxic lung adenocarcinoma cells: Mechanism of cell survival in solid tumor core. *American Journal of Physiology-Cell Physiology*, *289*(4), C918–C933.
- Langhans, S. A. (2018). Three-dimensional in vitro cell culture models in drug discovery and drug repositioning. *Frontiers in Pharmacology*, *9*, 6.
- Laschke, M. W., & Menger, M. D. (2016). Prevascularization in tissue engineering: Current concepts and future directions. *Biotechnology Advances*, *34*(2), 112–121.
- Laschke, M. W., & Menger, M. D. (2017). Spheroids as vascularization units: From angiogenesis research to tissue engineering applications. *Biotechnology Advances*, *35*(6), 782–791.
- Lee, P. J., & Choi, A. M. K. (2003). Pathways of cell signaling in hyperoxia. *Free Radical Biology and Medicine*, *35*(4), 341–350.
- Luo, Z., Tian, M., Yang, G., Tan, Q., Chen, Y., Li, G., Zhang, Q., Li, Y., Wan, P., & Wu, J. (2022). Hypoxia signaling in human health and diseases: Implications and prospects for therapeutics. *Signal Transduction and Targeted Therapy*, *7*(1), 218.
- Majmundar, A. J., Wong, W. J., & Simon, M. C. (2010). Hypoxia-inducible factors and the response to hypoxic stress. *Molecular Cell*, *40*(2), 294–309.
- Medina-Leyte, D. J., Domínguez-Pérez, M., Mercado, I., Villarreal-Molina, M. T., & Jacobo-Albavera, L. (2020). Use of human umbilical vein endothelial cells (HUVEC) as a model to study cardiovascular disease: A review. *Applied Sciences*, *10*(3), 938.
- Michiels, C. (2004). Physiological and pathological responses to hypoxia. *The American Journal of Pathology*, *164*(6), 1875–1882.
- Park, H.-J., Zhang, Y., Georgescu, S. P., Johnson, K. L., Kong, D., & Galper, J. B. (2006). Human umbilical vein endothelial cells and human dermal microvascular endothelial cells offer new insights into the relationship between lipid metabolism and angiogenesis. *Stem cell reviews*, *2*(2), 93–101.
- Sambale, F., Lavrentieva, A., Stahl, F., Blume, C., Stiesch, M., Kasper, C., Bahnmann, D., & Scheper, T. (2015). Three dimensional spheroid cell culture for nanoparticle safety testing. *Journal of Biotechnology*, *205*, 120–129.
- Schmitz, C., Pepelanova, I., Seliktar, D., Potekhina, E., Belousov, V. V., Scheper, T., & Lavrentieva, A. (2020). Live reporting for hypoxia: Hypoxia sensor-modified mesenchymal stem cells as in vitro reporters. *Biotechnology and Bioengineering*, *117*(11), 3265–3276.
- Schmitz, C., Potekhina, E., Irianto, T., Belousov, V. V., & Lavrentieva, A. (2021). Hypoxia onset in mesenchymal stem cell spheroids: Monitoring with hypoxia reporter cells. *Frontiers in Bioengineering and Biotechnology*, *9*, 611837.
- Tien, J. (2011). Tissue engineering of the microvasculature. *Comprehensive Physiology*, *9*(3), 1155–1212.
- Tucker, W. D., Arora, Y., & Mahajan, K. (2022). Anatomy, blood vessels. StatPearls Publishing. <https://pubmed.ncbi.nlm.nih.gov/29262226/>
- Vajda, J., Milojević, M., Maver, U., & Vihar, B. (2021). Microvascular tissue engineering—A review. *Biomedicines*, *9*(6), 589.
- Wang, Z., Mithieux, S. M., & Weiss, A. S. (2019). Fabrication techniques for vascular and vascularized tissue engineering. *Advanced Healthcare Materials*, *8*(19), 1900742.
- Weber, G. F., Bjerke, M. A., & DeSimone, D. W. (2011). Integrins and cadherins join forces to form adhesive networks. *Journal of Cell Science*, *124*(8), 1183–1193.
- Zhou, L., Dosanjh, A., Chen, H., & Karasek, M. (2000). Divergent effects of extracellular oxygen on the growth, morphology, and function of human skin microvascular endothelial cells. *Journal of Cellular Physiology*, *182*(1), 134–140.

## SUPPORTING INFORMATION

Additional supporting information can be found online in the Supporting Information section at the end of this article.

**How to cite this article:** Dienemann, S., Schmidt, V., Fleischhammer, T., Mueller, J. H., & Lavrentieva, A. (2023). Comparative analysis of hypoxic response of human microvascular and umbilical vein endothelial cells in 2D and 3D cell culture systems. *Journal of Cellular Physiology*, *238*, 1111–1120. <https://doi.org/10.1002/jcp.31002>